

Parity Violation in $\vec{p}p$ and $\vec{n}p$ Experiments

W.D. Ramsay

*Department of Physics and Astronomy,
University of Manitoba, Winnipeg, MB, R3T 2N2, Canada*

November 3, 2018

Abstract

Parity violation experiments involving only two nucleons provide a way to study the non-leptonic, strangeness-conserving part of the weak interaction in a clean measurement free of nuclear structure uncertainties. Such measurements are particularly appropriate for discussion at this conference as their success depends critically on the ability to accurately control and measure spin. Although simple in principle, the experiments are technically very demanding and great pains must be taken both in the preparation of the incident polarized beams and the measurement of the resultant parity violating asymmetries, which may be masked by a multitude of systematic effects. At low and intermediate energies, $\vec{p}p$ experiments are sensitive to the medium range part of the parity violating nucleon-nucleon force, usually parameterized in terms of rho and omega meson exchange. The pion does not contribute to parity violation in the pp experiments, as the π^0 is its own antiparticle and parity violation would also imply CP violation. I review existing pp measurements with particular emphasis on the recent 221 MeV $\vec{p}p$ measurement at TRIUMF which permitted the weak meson-nucleon coupling constants h_ρ^{pp} and h_ω^{pp} to be determined separately for the first time. The $\vec{n}p$ experiments, on the other hand, are used to extract the weak pion nucleon coupling, f_π , describing the longest range part of the parity violating nucleon-nucleon force. The np system is the only two nucleon system that is sensitive to f_π . I also review these experiments, with specific details of the $\vec{n}p \rightarrow d\gamma$ experiment now under preparation at Los Alamos National Laboratory.

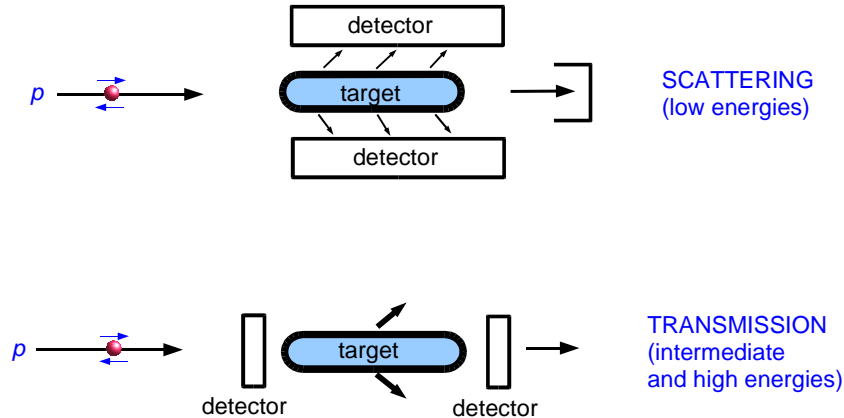


Figure 1: Types of $\vec{p}p$ experiments. The low-energy experiments use scattering geometry, while the intermediate and high-energy experiments use transmission geometry.

1 Introduction

Sometimes it is necessary to repeat what we know. All mapmakers should place the Mississippi at the same location, and avoid originality. – Saul Bellow

In preparing a review talk, one becomes acutely aware of essentially “repeating what we know”. In this review I will, however, do just that, concentrating in particular on what we know about pp and np parity violation experiments in which we control the spin of the incident nucleon, in other words experiments that use the nucleon spin as a tool, rather than experiments concerned with the nature of the nucleon spin itself. I will give a historical overview of $\vec{p}p$ and $\vec{n}p$ parity violation experiments, with technical details of the experiments I am most familiar with – the TRIUMF 221 MeV $\vec{p}p$ experiment and the Los Alamos $\vec{n}p \rightarrow d\gamma$ experiment now being installed at LANSCE. What I cover is a biased personal selection, and I refer readers interested in more background to two fine reviews of the field by Adelberger and Haxton [1] and Haeberli and Holstein [2].

1.1 Parity and the Weak Interaction

The parity operation reflects all space coordinates through the origin ($\vec{r} \rightarrow -\vec{r}$), which is equivalent to a mirror reflection (which reverses only one space

coordinate)¹ and a 180⁰ rotation (which reverses the other two). Since we can assume rotational invariance, the parity operation is often thought of as simply a mirror reflection. If a process is not identical to its mirror image, it is said to be parity violating (PV) or parity nonconserving (PNC). In physics, parity violation is exclusive to processes involving the weak interaction, such as:

1. $\mu \rightarrow e^- + \nu_\mu \bar{\nu}_e$
2. $n \rightarrow p + e^- + \bar{\nu}_e$; $\Lambda \rightarrow p + e^- + \bar{\nu}_e$
3. $K^+ \rightarrow \pi^+ \pi^-$
4. $pp \rightarrow pp$

The first three examples, in the leptonic, semi-leptonic and hadronic $\Delta s = 1$, sectors, clearly involve the weak interaction; the decays shown would disappear without it. The last example, however, in the purely hadronic $\Delta s = 0$ sector, is so dominated by the strong interaction that, were the weak interaction to disappear, the process would be virtually unchanged. The only way to see the effects of the weak interaction in such processes is to look for parity violation, and the experimental signal is very small. In pp scattering, for example, the parity violating part of the scattering cross section is typically of order 10^{-7} of the parity conserving part.

2 $\vec{p}p$ Experiments

Figure 1 shows typical $\vec{p}p$ parity violation experiments. They scatter a longitudinally polarized beam of protons from a hydrogen target and measure the difference in cross section for right-handed and left-handed proton helicities. The low energy experiments use scattering geometry, in which the detectors measure the scattered protons directly. The intermediate and high energy experiments use transmission geometry in which the change in scattering cross section is deduced from the change in transmission through the target. Transmission geometry uses a simpler detector arrangement, but can't be used at low energies because the energy loss in the target is too high to permit a sufficiently thick target. The quantity reported by both types of experiments is the parity violating longitudinal analyzing power, $A_z = \frac{\sigma^+ - \sigma^-}{\sigma^+ + \sigma^-}$, where σ^+ and σ^- are the scattering cross sections for positive and negative

¹The answer to your kids' question, "Why does a mirror reverse left-right but not up-down?" is that it doesn't; it reverses fore and aft. You do the left-right reversal when you turn the paper around to look at it in the mirror.

helicity. Because the statistical precision required on A_z is typically $\pm 10^{-8}$, it would take too long to count the requisite 10^{16} scattered particles, and all $\vec{p}p$ experiments so far have used current mode detection (as opposed to counting individual scattered particles).

2.0.1 Historical Summary

A roughly historical summary of $\vec{p}p$ parity violation experiments is given in Table 1. The long time taken to acquire measurements at a reasonable selection of energies and with small experimental uncertainties reflects the technical difficulty of these measurements. Running time is dominated by the time required to understand, and correct for, the various sources of systematic error. The time required to get the desired statistical precision is normally small by comparison.

Lab/Energy	Technical Details	A_z (10^{-7})	Where Reported
Los Alamos 15 MeV	scattering	$+1 \pm 4$	1974 Phys. Rev. Lett. [3]
	3 atm x 38cm hydrogen gas 4 liquid scintillators		
	scattering	-1.7 ± 0.8	1978 Argonne Conference [4]
	6.9 atm hydrogen gas 4 plastic scintillators		
Texas A&M 47 MeV	scattering	-4.6 ± 2.6	1983 Florence Conference [5]
	39 atm x 42cm hydrogen gas 4 plastic scintillators		
Berkeley 46 MeV	scattering	-1.3 ± 1.1	1980 Santa Fe Conference [6]
	80 atm hydrogen gas target He ion chamber around target		
SIN (PSI) 45 MeV	scattering	-1.63 ± 1.03	1985 Osaka Conference [7]
	100 atm hydrogen gas annular ion chamber	-3.2 ± 1.1	1980 Phys. Rev. Lett. [8]
		-2.32 ± 0.89	1984 Phys. Rev. D. [9]
		-1.50 ± 0.22	1987 Phys. Rev. Lett. [10]
Los Alamos 800 MeV	transmission	$+2.4 \pm 1.1$	1986 Phys. Rev. Lett. [11]
	1 m liquid hydrogen gas ion chambers		
Bonn 13.6 MeV	scattering	-1.5 ± 1.1	1991 Phys. Lett. B [12]
	15 atm hydrogen gas hydrogen ion chambers		
		-0.93 ± 0.21	1994 private communication [13]
TRIUMF 221 MeV	transmission	$+0.84 \pm 0.34$	2001 Phys. Rev. Lett. [14]
	40 cm liquid hydrogen hydrogen ion chambers		
Argonne ZGS 5130 MeV	transmission	$+26.5 \pm 7.0$	1986 Phys. Rev. Lett. [15]
	81 cm water target ion chambers and scintillators		

Table 1: Summary of $\vec{p}p$ parity violation experiments. The long times taken to achieve small uncertainties reflects the time taken to understand and correct for systematic errors. In cases where authors reported both statistical and systematic uncertainties, this table shows the quadrature sum of the two.

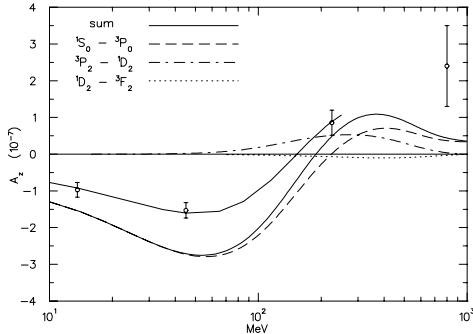


Figure 2: Partial wave decomposition of A_z . The broken curves and lower solid sum curve are calculated by Driscoll and Miller [23] using the DDH best guess couplings [16]. The upper solid sum curve is calculated by Carson *et al.* [24] with adjusted couplings.

2.0.2 Interpretation of the Results

Although it is known that the weak force is carried by the W and Z bosons, it is also known that their range is very small ($\sim 0.002 fm$), and most authors assume that at low and intermediate energies the protons never get close enough for direct W and Z exchange. The interaction is normally treated in a meson exchange model with one strong, parity conserving vertex and one weak, parity non-conserving vertex. The weak vertex is parameterized in terms of a set of weak meson-nucleon coupling constants, $f_\pi, h_\rho^{0,1,2}, h_\omega^{0,1}$, where the subscript denotes the exchanged meson and the superscript gives the isospin change [16]. Mesons heavier than the ω -meson are not included because of the hard core of the nucleon-nucleon force. Further, for the pp interaction there is no π exchange because the π^0 is its own antiparticle and parity violation would also imply CP violation, another factor of 10^3 suppression. CP invariance also excludes other neutral scalar and pseudoscalar mesons such as the $\eta, \eta', S,$ and δ^0 from consideration (Barton's theorem [17]).

The weak couplings were calculated by Desplanques, Donoghue and Holstein [16], and subsequently by a number of other authors [18, 19, 20, 21, 22]. The range of calculated values is large, and an experimental determination is needed.

Figure 2 shows A_z as a function of energy, broken down into contributions from various partial wave mixings [23]. Since the parity is $(-1)^\ell$, where ℓ is the orbital angular momentum, one would not normally expect partial

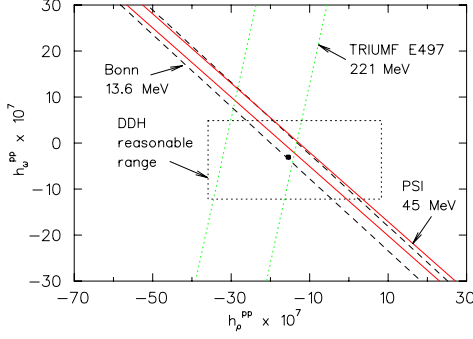


Figure 3: Constraints on the weak meson-nucleon couplings imposed by experiments in the energy range where the meson exchange model is normally used. The bands are based on calculations by Carlson *et al.* [24] using the AV18 potential [25] and CD-Bonn strong couplings [26]. (Figure modified from [14])

waves differing by one unit in ℓ (S-P, P-D, etc.)² to mix, but due to the weak force, some small mixing occurs. At low energy, A_z is dominated by the contribution of S-P mixing. At the energy of the TRIUMF experiment, A_z arises almost exclusively from P-D mixing. The *shape* of the curves is set by the strong interaction, while the multiplying factor is set by the weak interaction. By adjusting the multiplying factors to fit the data, the weak meson-nucleon couplings can be extracted. The lower solid line is the total A_z calculated by Driscoll and Miller [23] using the DDH [16] weak couplings. The upper solid line is from a calculation by Carlson *et al.* [24] using adjusted values of the weak couplings.

pp experiments are sensitive to the combinations $h_\rho^{pp} = h_\rho^{(0)} + h_\rho^{(1)} + \frac{1}{\sqrt{6}}h_\rho^{(2)}$ and $h_\omega^{pp} = h_\omega^{(0)} + h_\omega^{(1)}$. Using the AV18 strong potential [25] and CD-Bonn values for the strong couplings [26], Carlson *et al.* [24] calculate that

$$\begin{aligned} A_z(13.6\text{MeV}) &= 0.059h_\rho^{pp} + 0.075h_\omega^{pp} \\ A_z(45\text{MeV}) &= 0.10h_\rho^{pp} + 0.14h_\omega^{pp} \\ A_z(225\text{MeV}) &= -0.038h_\rho^{pp} + 0.010h_\omega^{pp} \end{aligned}$$

These constraints are shown graphically in Fig. 3. Notice that the precision results from Bonn and PSI determine essentially the same combination of couplings.

²The notation in Fig. 2 is $(2S+1)\ell_J$, where S is the total spin (0 or 1), $\ell = \text{S,P,D,F}$ is orbital angular momentum of 0,1,2,3, and J is the total angular momentum.

Table 2: Overall corrections for systematic errors. The table shows the average value of each coherent modulation, the net correction made for this modulation, and the uncertainty resulting from applying the correction.

Property	Average Value	$10^7 \Delta A_z$
$A_z^{uncorrected}(10^{-7})$	$1.68 \pm 0.29(stat.)$	
$y * P_x(\mu m)$	-0.1 ± 0.0	-0.01 ± 0.01
$x * P_y(\mu m)$	-0.1 ± 0.0	0.01 ± 0.03
$\langle yP_x \rangle(\mu m)$	1.1 ± 0.4	0.11 ± 0.01
$\langle xP_y \rangle(\mu m)$	-2.1 ± 0.4	0.54 ± 0.06
$\Delta I/I(ppm)$	15 ± 1	0.19 ± 0.02
<i>position + size</i>		0 ± 0.10
$\Delta E(meV at OPPIS)$	7–15	0.0 ± 0.12
electronic crosstalk		0.0 ± 0.04
Total		$0.84 \pm 0.17(syst.)$
$A_z^{corr}(10^{-7})$	$0.84 \pm 0.29(stat.) \pm 0.17(syst.)$	
$\chi^2_\nu(23sets)$	1.08	

The TRIUMF pp experiment [14] is a transmission experiment, as depicted in the bottom panel of Fig. 1. A 221 MeV longitudinally polarized proton beam was passed through a 40 cm long liquid hydrogen target, which scattered about 4% of the beam. Hydrogen filled ion chambers located upstream and downstream of the target measured the change in transmission when the spin of the incident protons was flipped from right-handed to left-handed. Although a very good optically pumped polarized ion source [27, 28, 29] was used that minimized the changes in beam properties other than helicity, other beam properties still change very slightly. These helicity-correlated beam property changes cause a systematic shift in the A_z distribution, and corrections must be made. To do this, the TRIUMF group continuously measured the helicity correlated changes in beam properties and made corrections based on the sensitivities determined in separate control measurements. The data before and after correction are shown in Fig. 4. The main effect visible to the eye is from *first moments of transverse polarization* resulting from the distribution of transverse polarization components across the beam. All the corrections are summarized in Table 2. The measured A_z actually came half from true parity violation and half from false effects.

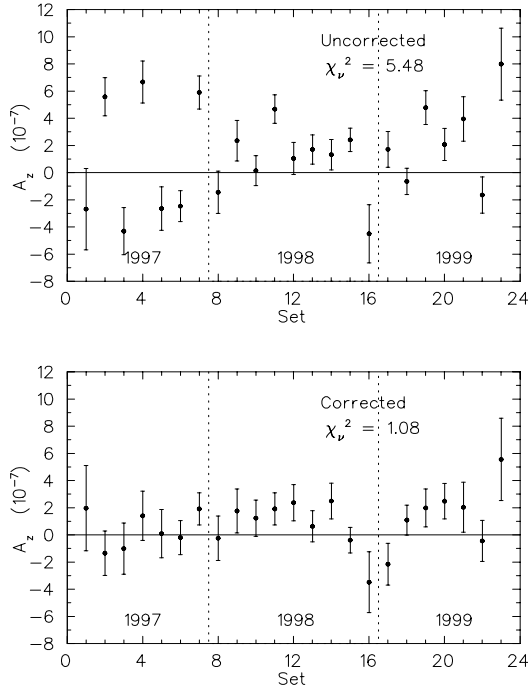


Figure 4: Effect of corrections to the E497 data. The main effect visible to the eye is for first moments of transverse polarization.

3 $\vec{n}p \rightarrow d\gamma$ Experiments

Unlike the $\vec{p}p$ experiments just discussed, which are sensitive to ρ and ω exchange, $\vec{n}p \rightarrow d\gamma$ experiments are sensitive almost exclusively to pion exchange, and measure the weak pion-nucleon coupling, f_π .³ Measurements such as the circular γ -ray polarization from ^{21}Ne [30], or the longitudinal analyzing power in $p\alpha$ scattering [31], provide constraints on a combination of π , ρ , and ω couplings. The most precise limit on f_π alone is believed to be from measurements of circularly polarized gamma rays from a parity mixed doublet in ^{18}F [32, 33]. These results, however, are only about 10% of theoretical predictions [16, 34, 35], which give $f_\pi \sim 4 \times 10^{-7}$, and are also at odds with the large value of f_π deduced from measurements of the anapole moment in ^{133}Cs [36, 37], although the ^{133}Cs experiment is also sensitive to $h_\rho^{(0)}$, and, as pointed out by Wilburn and Bowman, [38] the disagreement may not be too significant.

$np \rightarrow d\gamma$ radiative capture measurements can be made with unpolarized neutrons, as was done in the Leningrad experiment [39], but the circular

³Some authors quote $H_\pi = f_\pi \frac{g_\pi}{\sqrt{32}}$, where g_π is the strong pion-nucleon coupling.

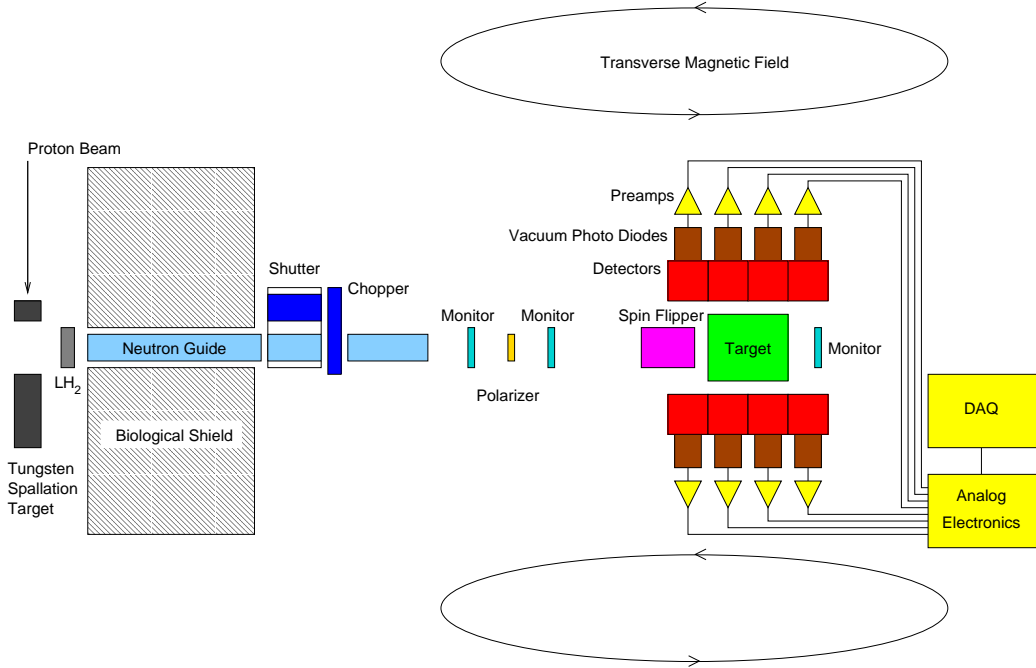


Figure 5: Layout of apparatus for the $\vec{n}p \rightarrow d\gamma$ experiment at LANSCE.

polarization, P_γ , of the capture gammas must be measured and the analyzing power of the polarimeters is very low. In an $\vec{n}p \rightarrow d\gamma$ experiment, the incident cold neutrons are polarized vertically and the gamma rays produced by neutron capture in the hydrogen target are expected to be emitted slightly more in the direction opposite to the neutron spin. The up-down asymmetry $A_\gamma \approx -0.11f_\pi$ provides a clean measure of f_π free of nuclear structure uncertainties [40]. Previous measurements at ILL Grenoble gave $A_\gamma = (6 \pm 21) \times 10^{-8}$ [41] and $A_\gamma = (-1.5 \pm 4.8) \times 10^{-8}$ [42], but neither result was accurate enough to impose a significant constraint.

An experiment is now being prepared at Los Alamos to measure the gamma ray asymmetry in $\vec{n}p \rightarrow d\gamma$ with an uncertainty of $\pm 0.5 \times 10^{-8}$ [40]. The expected asymmetry is $A_\gamma \approx -5 \times 10^{-8}$.

The apparatus is shown schematically in Fig. 5. A pulsed, 800 MeV, 100-150 μA proton beam impinges on a tungsten spallation target. Neutrons from the spallation target are cooled in a liquid hydrogen moderator and transported to the experiment in a neutron guide. The neutron guide prevents the $1/r^2$ intensity fall-off that would otherwise occur, and also enhances the fraction of low energy neutrons. The peak neutron flux through the 9.5 cm x 9.5 cm guide is 6×10^7 n/ms at 8 meV.

The neutrons are polarized by passing through a polarized ^3He spin filter. Neutrons with spin parallel to the ^3He spin pass through the filter, while neutrons with spin anti-parallel to the ^3He spin are captured. The neutron polarization is determined by the front monitors located before and after the spin filter. If half the neutrons are captured, the polarization of the downstream neutron beam is 100%. A test ^3He spin filter was demonstrated in a fall 2000 test run and the final version will be tested at the University of Michigan in fall 2002.

The polarized neutrons are captured in a 30 cm long, 20 L liquid para-hydrogen target operating at 17 K. The low temperature is important to keep a small (0.03%) equilibrium ortho-hydrogen fraction, as the spin 1 ortho-hydrogen molecule allows spin-flip scattering and destroys the asymmetry. The cross section for scattering from ortho-hydrogen is approximately 20 times that for scattering from para-hydrogen, so the neutron detector downstream of the target will indicate any change in the ortho-hydrogen fraction. Approximately 60% of the neutrons are captured in the para-hydrogen, producing a deuteron and a 2.2 MeV gamma ray. The gamma rays are measured by an array of 48 $15 \times 15 \text{ cm}^2$ CsI(Tl) detectors surrounding the target.

The neutron spin is flipped 20 times per second by a 30 kHz RF spin filter. The RF itself has a very small ($< 0.1 \text{ mm}$) skin depth in, and is well contained by, the conducting shell surrounding the spin filter. In the fall 2000 test runs at LANSCE, the on-axis spin flipper efficiency was $\approx 95\%$.

The neutron beam is pulsed at 20 Hz, so the data acquisition operates in 50 ms “frames”. The pulsed beam makes it possible to identify neutrons by their time of flight over the 22 m flight path. The fast neutrons arrive at the target first, and for the first 9 ms the neutron energy is above the 15 meV required to excite a para-to-ortho transition in the para-hydrogen target. For this reason, the first 9 ms of a frame will have no physics asymmetry and can be used to measure background. From 9 ms to 30 ms, the neutron energy falls from 15 meV to 1.5 meV. The amplitude of the RF spin filter is synchronized with this fall to ensure that fast and slow neutrons are all rotated by 180° . After 40 ms, a “frame overlap chopper” blocks the neutrons so that slow neutrons from one frame are not still arriving when fast neutrons from the next pulse arrive. During the 40 ms to 50 ms dead interval, electronic noise can be checked. Different systematic errors have a different dependence on neutron energy and their time-of-flight signatures can be used to identify them. In addition, the ^3He spin filter direction and the overall holding field can be reversed for further cancellation of systematic errors.

The beamline, FP12, is now almost complete at LANSCE. The experimental cave is scheduled for installation in early 2003 and commissioning runs are planned for summer and fall of 2003.

4 Summary

pp and np parity violation experiments provide a means to study the hadronic, $\Delta s = 0$ part of the weak interaction. $\vec{n}p \rightarrow d\gamma$ experiments are sensitive to the long range part of the nucleon-nucleon interaction and constrain the weak pion-nucleon coupling constant, f_π . Despite decades of experimental and theoretical work, the strength of this coupling is still very uncertain. The new, precision experiment now under construction at the LANSCE pulsed neutron source at Los Alamos should finally lay this question to rest. $\vec{p}p$ parity violation experiments are sensitive to the shorter range part of the nucleon-nucleon force and constrain the combinations $h_\rho^{pp} = h_\rho^{(0)} + h_\rho^{(1)} + \frac{1}{\sqrt{6}}h_\rho^{(2)}$ and $h_\omega^{pp} = h_\omega^{(0)} + h_\omega^{(1)}$. Prior to 2001, low energy experiments had constrained only a linear combination of approximately equal parts h_ρ^{pp} and h_ω^{pp} . With the addition of the TRIUMF 221 MeV result in 2001, h_ρ^{pp} and h_ω^{pp} are now separately constrained. The data so far are not sufficient to determine all 6 couplings, $f_\pi, h_\rho^{0,1,2}, h_\omega^{0,1}$, and much careful experimental work remains to be done. Nonetheless, one should remember that, in the words of Charles Babbage, “errors using inadequate data are much less than those using no data at all”.

References

- [1] E.G. Adelberger and W.C. Haxton, *Ann. Rev. Nucl. Part. Sci.* **35**, 501 (1985).
- [2] W. Haeberli and Barry R. Holstein, in *Symmetries and Fundamental Interactions in Nuclei*, edited by W.C. Haxton and E.M. Henley, (World Scientific, 1995) p. 17.
- [3] J.M. Potter *et al.*, *Phys. Rev. Lett.* **33**, 1307 (1974).
- [4] D.E. Nagle *et al.*, in *Proceedings of the 3rd International Conference on High Energy Beams and Polarized Targets* (Argonne, 1978), edited by L.H. Thomas, AIP Conference Proceedings 51, New York 1979, p. 224.
- [5] D.M. Tanner *et al.*, in *Proceedings of the International Conference on Nuclear Physics* (Florence, 1983), (Typographia, Bologna, 1983), p. 697.
- [6] P. von Rossen *et al.*, in *Proceedings of the 5th International Symposium on Polarization Phenomena in Nuclear Physics* (Santa Fe, 1980), edited by G.G. Ohlsen *et al.*, AIP Conference Proceedings 69, New York, 1981, p. 1442.

- [7] P. von Rossen *et al.*, in *Proceedings of the 6th International Symposium on Polarization Phenomena in Nuclear Physics* (Osaka, 1985), J. Phys. Soc. Japan **55**, Suppl. p. 1016 (1986).
- [8] R. Balzer *et al.*, Phys. Rev. Lett. **44**, 699 (1980).
- [9] R. Balzer *et al.*, Phys. Rev. C **30**, 1409 (1984).
- [10] S. Kistryn *et al.*, Phys. Rev. Lett. **58**, 1616 (1987).
- [11] V. Yuan *et al.*, Phys. Rev. Lett. **57**, 1680 (1986).
- [12] P.D. Eversheim *et al.*, Phys. Lett. B **256**, 11 (1991)
- [13] P.D. Eversheim, private communication (1994).
- [14] A.R. Berdoz *et al.*, Phys. Rev. Lett. **87**, 272301 (2001).
- [15] N. Lockyer *et al.*, Phys. Rev. D **30**, 860 (1984).
- [16] B. Desplanques, J.F. Donoghue, and B.R. Holstein, Ann. Phys.(N.Y.) **124**, 449 (1980).
- [17] G. Barton, Nuovo Cimento **19**, 512 (1961).
- [18] V.M. Dubovik and S.V. Zenkin, Ann. Phys.(N.Y.) **172**, 100 (1986).
- [19] G.B. Feldman, G.A. Crawford, J. Dubach, and B.R. Holstein, Phys. Rev. C **43**, 863 (1991).
- [20] N. Kaiser and U-G. Meissner, Nucl. Phys. A **499**, 699 (1989).
- [21] U-G. Meissner and N. Kaiser, Nucl. Phys. A **510**, 759 (1990).
- [22] U-G. Meissner and H. Wiegel, Phys. Lett. B **447**, 1 (1999).
- [23] D.E. Driscoll and G.A. Miller, Phys. Rev. C **39**, 1951 (1989); *ibid.*, **40**, 2159 (1989).
- [24] J.A. Carlson, R. Schiavilla, V.R. Brown, and B.F. Gibson, Phys. Rev. C **65**, 035502, (2002); R. Schiavilla, private communication (2001).
- [25] R.B. Wiringa, *et al.*, Phys. Rev. C **51**, 38 (1995).
- [26] R. Machleidt, Phys. Rev. C **63**, 24001 (2001).

- [27] A.N. Zelenski *et al.*, in *Proceedings of the 12th International Symposium on High Energy Spin Physics (SPIN96)*, edited by C.W. de Jager *et al.*, (World Scientific, Amsterdam, 1997), p. 637.
- [28] A.N. Zelenski *et al.*, in *Proceedings of the 6th Conference on Intersections Between Particle and Nuclear Physics*, edited by T.W. Donnelly, AIP Conference Proceedings 412, New York, 1997, p.328.
- [29] C.D.P. Levy *et al.*, in *Proceedings of the International Workshop on Polarized Beams and Polarized Gas Targets* (Cologne, 1995), edited by H.P. gen. Schieck and L. Sydow (World Scientific, Singapore, 1996), p. 120; A.N. Zelenski, *ibid.*, p. 111.
- [30] E.D. Earle *et al.*, Nucl. Phys. A **396**, 221 (1983).
- [31] J. Lang *et al.*, Phys. Rev. C **34**, 1545 (1986).
- [32] S.A. Page *et al.*, Phys.Rev. **C35**, 1119 (1987).
- [33] M. Bini *et al.*, Phys. Rev. Lett. **55**, 795 (1985).
- [34] D.B. Kaplan and M.J. Savage, Nucl. Phys. A **556**, 653 (1993).
- [35] E.M. Henley *et al.*, Phys. Lett. B **440**, 449 (1998).
- [36] C.S. Wood *et al.*, Science **275**, 1759 (1997).
- [37] V.V. Flambaum and D.W. Murray, Phys. Rev. C **56**, 1641 (1997).
- [38] W.S. Wilburn and J.D. Bowman, Phys. Rev. C **57**, 3425 (1998).
- [39] V.A. Knyazkov *et al.*, Nucl. Phys. A **417**, 209 (1984).
- [40] W.M. Snow *et al.*, Nucl. Inst. Meth. A **440**, 729 (2000).
- [41] J.F. Caviagnac *et al.*, Phys. Lett. B **67**, 148 (1977).
- [42] J. Alberi *et al.*, Can. J. Phys. **66**, 542 (1988).